Kinetic Effects of Quarternary Lidocaine Block of Cardiac Sodium Channels: A Gating Current Study

DOROTHY A. HANCK, JONATHAN C. MAKIELSKI, and MICHAEL F. SHEETS*

From the Department of Medicine and The Cardiac Electrophysiological Laboratories, University of Chicago, Chicago, Illinois 60637; and *The Department of Medicine and The Feinberg Cardiovascular Research Institute, Northwestern University Medical School, Chicago, Illinois 60611

ABSTRACT The interaction of antiarrhythmic drugs with ion channels is often described within the context of the modulated receptor hypothesis, which explains the action of drugs by proposing that the binding site has a variable affinity for drugs, depending upon whether the channel is closed, open, or inactivated. Lack of direct evidence for altered gating of cardiac Na channels allowed for the suggestion of an alternative model for drug interaction with cardiac channels, which postulated a fixed affinity receptor with access limited by the conformation of the channel (guarded receptor hypothesis). We report measurement of the gating currents of Na channels in canine cardiac Purkinje cells in the absence and presence of QX-222, a quarternary derivative of lidocaine, applied intracellularly, and benzocaine, a neutral local anesthetic. These data demonstrate that the cardiac Na channel behaves as a modulated rather than a guarded receptor in that drug-bound channels gate with altered kinetics. In addition, the results suggest a new interpretation of the modulated receptor hypothesis whereby drug occupancy reduces the overall voltage-dependence of gating, preventing full movement of the voltage sensor.

INTRODUCTION

Interactions of local anesthetics and antiarrhythmic drugs with ion channels have been explained within the context of the modulated receptor hypothesis (Hille, 1977; Hondeghem and Katzung, 1977). This model postulates that ion channels have a variable affinity for drugs based on the conformational state of the channel. For clinically useful class I antiarrhythmic drugs, kinetic states favored at hyperpolarized potentials (closed states) have a low affinity for drug compared with states favored at positive potentials (open and inactivated states), which have a higher affinity. Complex patterns of use-dependent block and recovery can be explained using this

Address correspondence to Dorothy A. Hanck, PhD, Cardiac Electrophysiology Laboratories (MC6094), University of Chicago, 5841 South Maryland Avenue, University of Chicago, Chicago, IL 60637.

model. However, even for models that contain a relatively small number of distinct channel conformations, the state diagram for a modulated receptor can be very complex because microscopic reversibility dictates that on and off rates for drug binding to the various states be balanced by changes in the rate constants of gating of drug-bound vs drug-free channels. This important corollary of the modulated receptor hypothesis, altered gating of drug-bound channels, is difficult to verify from ionic current data alone because blocked channels, whether in the rested, open, or inactivated conformation, are all thought to be nonconducting. A direct test for altered gating can be made from gating currents (I_g), the small nonlinear capacitive currents that reflect the concerted motion of charges on the protein in response to voltage changes, because these occur for all voltage-dependent transitions, between both conducting and nonconducting states.

Altered gating of drug-bound channels has been noted for quaternary derivatives of lidocaine acting on Na channels in squid giant axon (Cahalan and Almers, 1979b; Tanguy and Yeh, 1989) and for procaine (Keynes and Rojas, 1974, but see Kniffki, Koppenhofer, and Vogel, 1976) and for trimecaine (Peganov and Khodorov, 1977, also see reviews Khodorov, 1981; Meves, 1990). However, one of the major limitations of the investigation of the effects of local anesthetics with Na channels in these noncardiac preparations has been the interaction of these agents with guanidinium toxins such as tetrodotoxin (TTX), which are used to reversibly block Na^+ permeation through the Na channel. For example, in squid giant axon whereas block of Na current (I_{Na}) by QX-314 was use-dependent, gating charge in the presence of TTX was reduced to 50% from "rest" (at the holding potential), i.e., pulsing was not required, and conditioning trains did not further reduce charge (Cahalan and Almers, 1979b). Only in the absence of TTX was charge from "rest" unaffected by the presence of 1 mM QX-314 and then reduced by ~50% after a conditioning pulse train. Similar findings have been reported for QX-572 and QX-314 in frog node of Ranvier (Guselnikova, Peganov, and Khodorov, 1979; Khodorov, 1981).

Until recently measurement of cardiac Na channel gating currents has not been possible. Lack of direct measurement of altered gating of drug-bound cardiac Na channels led to a simpler formulation of block by Starmer and colleagues (Starmer, Grant, and Strauss, 1984), who proposed that the binding site for drug could have a constant affinity and the apparent state dependency arose from the receptor being only transiently available. This model did not require that bound channels gate with altered kinetics so that drug on and off rates could be calculated from recurrence relations describing the response of I_{Na} in pulse trains.

Cardiac Na channel gating currents can now be measured (Hanck, Sheets, and Fozzard, 1990), and so this study was undertaken to investigate the kinetic consequences of local anesthetic block of cardiac Na channels by measuring Na channel I_g. We provide evidence based on the action of intracellularly applied QX-222 (QX-222$_i$) that drug-bound cardiac channels gate with altered kinetics in a manner similar to Na channels found in squid giant axon and frog node of Ranvier. However, whereas studies in those preparations have suggested that a portion of the gating charge becomes immobilized (i.e., a fraction of drug-bound channels do not gate over the time period of measurement) (Cahalan and Almers, 1979b; Cahalan, Shapiro, and Almers, 1980; Khodorov, 1981; Bekkers, Greeff, Keynes, and Neumcke, 1984;

Tanguy and Yeh, 1989), we find that all drug-bound channels continue to gate but with lower voltage dependency than drug-free channels. The reduced voltage dependency appears not to be a consequence of the charge on the QX-222 molecule because similar effects were seen with the neutral local anesthetic benzocaine. We, therefore, suggest a new interpretation of the modulated receptor theory. Instead of drug occupancy shifting the equilibrium between rested, open, and inactivated states to one that favors drug-bound inactivated (immobilized) channels, drug occupancy reduces the overall voltage dependence of gating by preventing full movement of the voltage sensor. Some of these data have been presented in abstract form (Hanck, Sheets, and Makielski, 1992).

MATERIALS AND METHODS

Cell Preparation

Cells were isolated from canine Purkinje fibers using the procedure of Sheets and co-workers (Sheets, January, and Fozzard, 1983). Free running fibers from both the right and left ventricle were cut into 2–3 mm segments and incubated in a shaking water bath (37°C) for 1.5–2 h in a modified Eagle's minimal essential medium (MEM) with 5 mg/ml Worthington type I collagenase. Fibers were washed in 150 mM K-glutamate, 5.7 mM $MgCl_2$, 0.12 mM EGTA, and 5 mM HEPES (pH 6.2) at 37°C. Fibers were then mechanically separated into single cells by application of shear force. Cells were stored at room temperature in MEM (pH 7.3), which contains 1.8 mM Ca, and were studied within 18 h.

Recording Technique, Solutions, and Experimental Protocols

Recordings were made using a large bore, double-barrelled glass suction pipette for both voltage clamp and internal perfusion as previously described (Makielski, Sheets, Hanck, January, and Fozzard, 1987). I_{Na} was measured with a virtual ground amplifier (Burr-Brown OPA-101) with a 5-MΩ feedback resistor connected to the outflow channel of the bath via a 3 M KCl bridge and Ag/AgCl$_2$ pellet. Voltage protocols, using locally written control programs (DH), were imposed from a 12-bit DA converter (Masscomp 5450, Concurrent Computer, Tinton Falls, NJ) over a 30/1 voltage divider. Data were filtered by the inherent response of the voltage-clamp circuit (corner frequency near 125 kHz) and recorded with a 16-bit AD converter on a Masscomp 5450 at 300 kHz. A fraction of the current was fed back to compensate for series resistance with a resulting primary charging time constant of less than 30 μs.

Cells were placed in the aperture of the pipette in a low Ca^{2+} solution and transferred to one of four experimental chambers where they were allowed to form a high resistance seal to the pipette about their circumference. After the cell had sealed to the pipette the cell membrane inside the pipette was disrupted with a manipulator-controlled platinum wire. Voltage control was assessed by evaluating the time course of the ionic current in steps (V_t) to −40 mV, the time course of the capacitive current in steps between −150 mV and −190 mV, and the negative slope region of the peak current-voltage relationship. During experiments cells typically were held at −150 mV, which in these cells insured full I_{Na} availability, and were depolarized once per second or once each 1.5 s for 10, 16.7, 25, or 50 ms. Pulse trains usually consisted of 130-step depolarizations of 10-ms duration to 0 mV from a holding potential of −150 mV once each 100 ms (10 Hz).

Control extracellular solution for I_{Na} measurements contained (in mM) 15 Na$^+$, 135 TMA$^+$, 2 Ca^{2+}, 4 Mg^{2+}, 150 MES$^-$, 12 Cl$^-$, and 10 HEPES (pH 7.2). For measurements of I_g Na$^+$ was replaced with TMA$^+$ and 10 μM saxitoxin (STX) (Calbiochem Corp., San Diego, CA) was

added. Unlike nerve (Cahalan and Almers, 1979b; Khodorov, 1981) the presence of gua-nidinium toxin did not affect the development of use-dependent reduction of charge by drug. Intracellular solution contained 150 TMA$^+$, 150 F$^-$, 10 EGTA, and 10 HEPES (pH 7.2). Changes in bath solution were achieved by placing the pipette, with the cell in place, adjacent to the inlet of one of four parallel experimental chambers.

For these studies we chose STX to block ionic current through the channel because we previously found good reversibility of block, i.e., block produced by this toxin could be washed out within 1–2 min of removal of toxin from the bath (Hanck et al., 1990). In addition, because it is effective at blocking the channel at about 10-fold lower concentrations than TTX, it was cost-effective to use a concentration about 1,000-fold the K_D and thereby effectively blocking ionic currents.

QX-222 (a kind gift of Astra Pharmaceuticals, Marlborough, MA) was added to the intracellular solution at concentrations between 0.05 and 1 mM. Greater than 4.5 minutes was allowed for the washin of QX-222 (typically between 5–6 min). We used a slow pipette perfusion rate that produced a two to three minute delay before the drug reached the cell, but in all cases cells were exposed to drug for at least 2 min before pulsing was begun. During solution changes cells were held quiescent at −150 mV in the Na$^+$ containing bath, and for I_g measurements just before the initiation of pulse trains, the cell was transferred to the Na$^+$-free, STX containing, solution.

We chose QX-222 for these experiments because in pilot experiments we determined that, even though it was relatively slow at producing block, at a given concentration it produced faster development of block than did QX-314. We determined that this was not because of a relatively fast off-rate. For example after producing block with trains only a small amount of recovery occurred even after several minutes. In addition, in washout experiments, only partial recovery from block could be obtained and this required tens of minutes.

Temperature was controlled using a Sensortek (Physiotemp Instruments, Inc., Clifton, NJ) TS-4 feedback-controlled thermoelectric stage mounted beneath the bath chamber and typically varied less than 0.5°C during an experimental set. Cells were studied between 11°C and 15°C.

To maximize the signal to noise ratio protocols contained four repetitions at each test voltage that were ¼ of a 60 Hz cycle out of phase; this practice aided in rejection of this frequency in the signal averaged data. However, the signal to noise ratio was sufficiently good that reliable measurements of I_g during trains could be made from single depolarizations.

Data Analysis

Data were capacity corrected using eight or 16 scaled current responses to steps between −150 mV and −190 mV. Leak resistance (R_L), taken as the reciprocal of the linear conductance between −190 and −110 mV, had a mean value of 90 MΩ ($n = 27$ cells, range 15 to 298 MΩ). Cell capacitance was measured from the integral of the current responses to voltage steps between −150 mV and −190 mV and was 89 pF ± 21 pF ($n = 27$).

Peak I_{Na} was taken as the mean of four data samples (over 16.67 μs) clustered around the maximal value of data digitally filtered at 5 kHz, leak corrected by the amount of the time-independent linear leak extrapolated from the currents elicited between −110 and −190 mV. For charge measurements data were leak corrected by the mean of the data between 6 and 10 ms ($V_t < 0$ mV) or between 4 and 6 ms ($V_t \geq 0$ mV) and integrated for 10 ms. Running integrals exhibited a stable plateau except occasionally at the most positive potentials when a small outward ionic current, which developed after a delay of several milliseconds, was present. For kinetic analyses I_g relaxations were trimmed, decimated by two, and fitted with a sum of exponentials with DISCRETE (Provencher, 1976) to determine the decay time constants, amplitudes, baselines, and standard errors of the estimate for fitted parameters. This program

provided a modified F-statistic that was used to evaluate the number of exponential components that best described the data.

Data were analyzed and graphed on a Masscomp 5520 or Masscomp 5450 computer using locally written programs (DH) or on a SUN Sparcstation (IPX or Sparc10) using SAS (Statistical Analysis System, Cary, NC). Fitting programs on the Masscomp or on the SUN used algorithms from the Numerical Algorithms Group library (NAG, Oxford, UK) or from SAS. Unless otherwise specified all summary statistics are expressed as means ± one standard deviation (SD). Regression parameters are reported as the estimate and the standard error of the estimate (SEE).

RESULTS

Phasic Reduction in Gating Charge and Block of I_{Na} by $QX-222_i$

The presence of STX to block ionic currents did not affect the development of use-dependent reduction in charge by $QX-222_i$ in canine cardiac Purkinje cells. This was quite different from squid giant axon and frog node of Ranvier, where addition of guanidinium toxins abolished phasic reduction of gating charge (Cahalan and Almers, 1979b; Khodorov, 1981). Fig. 1 shows data from one of five cells in which I_g was recorded after exposure to 0.5 mM $QX-222_i$.

In each cell Na channel I_g was recorded under control conditions (external solution containing 10 µM STX and all Na^+ replaced by TMA^+) and then after $QX-222_i$ was added to the intracellular solution (as described in the Materials and Methods). The upper left panel of Fig. 1 shows that under control conditions I_g's in the train were quite similar and the charge was unaffected by the rapid pulsing protocol (*lower left*). After addition of 0.5 mM $QX-222_i$, I_g became altered during the train; even by eye the phasic reduction of the initial amplitude of I_g is apparent (*upper right*). The reduction in charge is better seen in the running integrals of I_g (*lower, right*).

The reduction in charge on the first depolarization after exposure to $QX-222_i$ was small and variable. In five cells exposed to 0.5 mM $QX-222_i$ reduction in charge varied between 0 and 29%, and in another five cells exposed to 1 mM $QX-222_i$ reduction varied between 8 and 25%. The mean value for the two doses combined was 15% ± 10% ($n = 10$). To evaluate the accuracy with which we could measure a reduction in gating charge in the first depolarization, in three cells we made sequential measurements of charge during repetitive exposures to STX. In these three cells charge measurements differed by 5% ($n = 3$ exposures), 9% ($n = 4$ exposures), and 11% ($n = 4$ exposures). In contrast to the small and variable amount of reduction in charge in first depolarizations, the phasic reduction in gating charge in the presence of $QX-222_i$ during pulse trains was prominent (Fig. 2). The total reduction in charge in 0.5 mM $QX-222_i$ was 41 ± 10% ($n = 5$), and in 1 mM $QX-222_i$ it was 46% ± 3% ($n = 5$).

In order to compare the magnitude and time course of the reduction in charge to block of I_{Na} by $QX-222_i$ we performed similar experiments in the presence of Na_o and without STX. Representative I_{Na} data are shown in Fig. 3. Under control conditions and at a high pulse frequency of 10 Hz the reduction in I_{Na} was modest; in four cells the reduction of peak I_{Na} by the end of the pulse train was 12% ± 4%. In the presence of 0.5 mM $QX-222_i$ peak I_{Na} in the first depolarization after exposure to drug was reduced by 11% ± 3% ($n = 4$) and in the presence of 1 mM $QX-222_i$ by

Control   0.5 mM QX-222$_i$
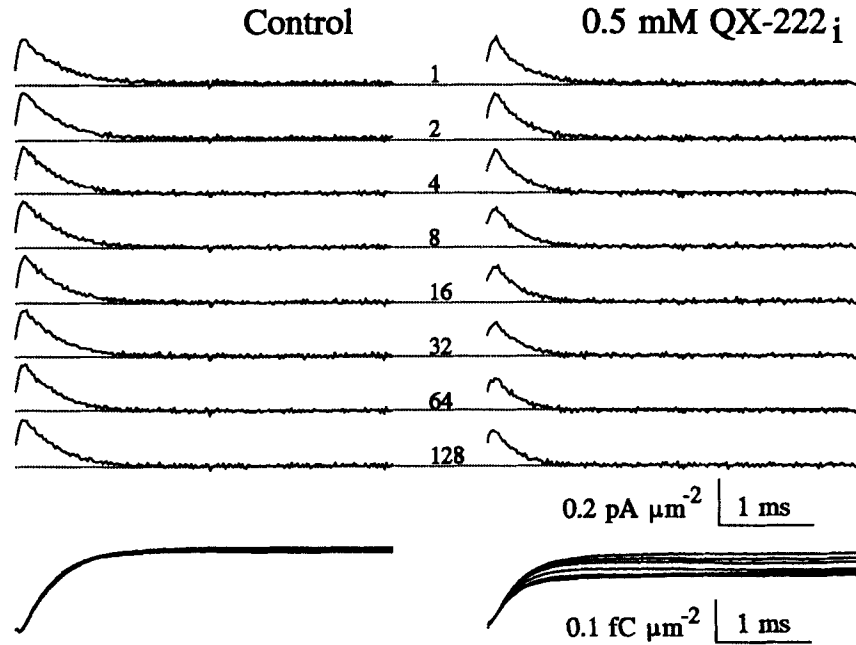

0.2 pA μm^{-2} | 1 ms

0.1 fC μm^{-2} | 1 ms

FIGURE 1. Nonlinear capacitive currents and charge recorded during a 10 Hz train of 130 pulses from a holding potential of −150 mV to a test potential of 0 mV for 10 ms. Upper traces show individual sweeps, corrected for linear capacitance, in control (*left*) and after exposure to 0.5 mM QX-222$_i$ (*right*). Lower panels show superimposed running integrals (charge) of the upper records. Note that the charge reached a plateau over the 4 ms graphed and that there was only a small reduction in charge in the first depolarization after exposure to drug. For graphing I$_g$ traces were digitally filtered at 20 kHz, and only every sixth point was plotted. Cell E7.05; R$_L$ 86 MΩ; 76 pF; 14°C.
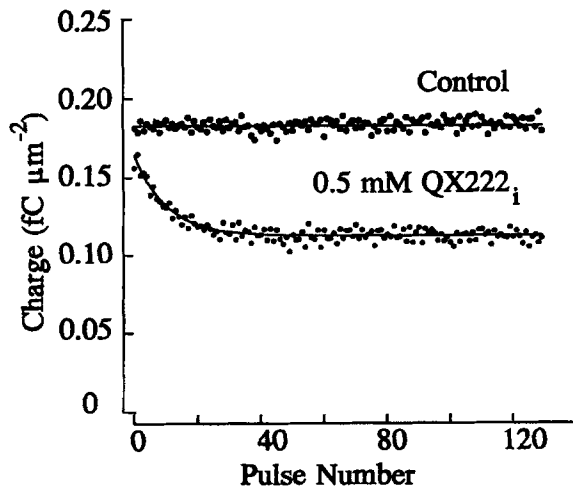

FIGURE 2. Reduction in gating charge during a 10 Hz train. Charge from the same cell shown in Fig. 1 is graphed. Whereas in control (O) charge was unaffected by the rapid pacing, after exposure to 0.5 mM QX-222$_i$ (●) charge showed phasic reduction during the train. The solid line is the best fit line (τ 9.9 pulses, amplitude 0.05 fC μm^{-2}, and 0.11 fC μm^{-2} remaining at the end of the train).
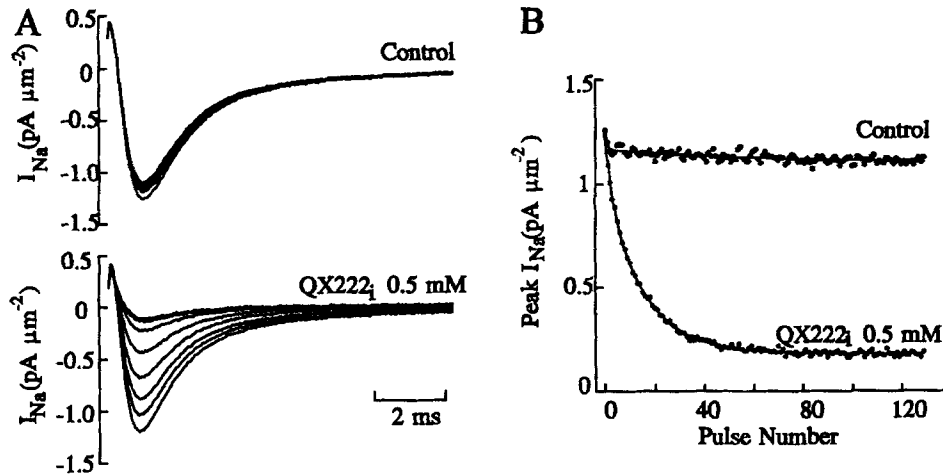
FIGURE 3.   Phasic block of I_{Na} in 10 Hz trains. (*A*) Capacity, but not leak corrected, currents during depolarizations to 0 mV for 10 ms from -150 mV in control (*upper*) and after exposure to 0.5 mM QX-222$_i$ (*lower*). Traces shown are the 1st, 2nd, 4th, 8th, 16th, 32nd, 64th, and 128th depolarization in the 130 pulse trains. (*B*) Peak I_{Na} measured from the trains and graphed vs pulse number. Solid lines were calculated from the parameters of the fits of the sum of exponentials to the data. Control: τ_{fast} 0.7 pulses; A_{fast} 0.09 pA μm^{-2}; τ_{slow} 80 pulses, A_{slow} 0.07 pA μm^{-2}. QX-222: τ_{fast} 2.5 pulses, A_{fast} 0.17 pA μm^{-2}; τ_{slow} 15 pulses, A_{slow} 0.8 pA μm^{-2}. Cell E7.03; R_L 56 MΩ; 101 pF; 14°C.
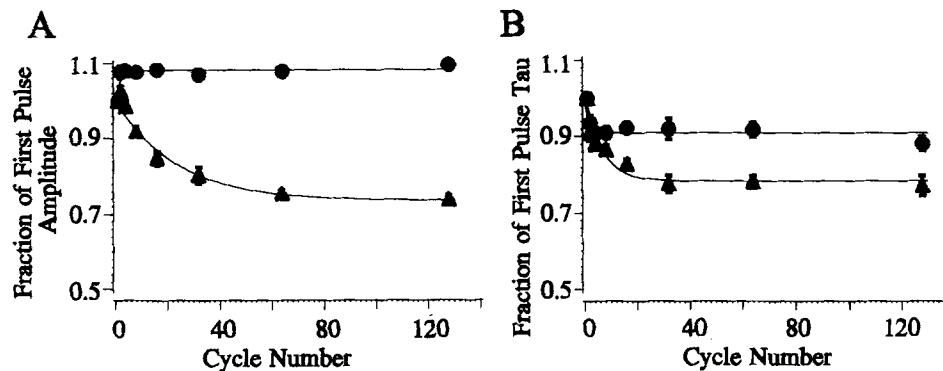

FIGURE 4.   Effect of QX-222$_i$ on the amplitude and time constant of I_g relaxations during 10 Hz pulse trains to 0 mV from a holding potential of -150 mV. Individual I_g sweeps were capacity corrected, trimmed, decimated by two and fit with up to three exponentials as described in the text. In all cases at least 9.7 ms of data were fitted. Means $\pm$ SEM are graphed for the relative values for the 1st, 2nd, 4th, 8th, 16th, 32nd, 64th, and 128th sweeps in 130 pulse trains for ten cells (five exposed to 0.5 mM QX-222$_i$ and 5 exposed to 1 mM QX-222$_i$). (*A*) Reduction in initial amplitude of I_g in control (○) and in QX-222$_i$ (▲). Each data value was calculated as the fraction of the value in the first depolarization. (*B*) Abbreviation of the time constant of I_g relaxation in control (○) and in QX-222$_i$ (▲) calculated as the fraction of the value in the first depolarization. Mean value of the first τ in the train was 0.38 $\pm$ 0.05 ms in control and 0.29 ms $\pm$ 0.04 ms ($n = 10$) in drug. Last pulse in control was 0.33 $\pm$ 0.05 ms and 0.22 $\pm$ 0.02 ms in drug ($n = 10$).

17% ± 5% (n = 4). At the end of the 130 pulse 10 Hz trains in the presence of 0.5 mM QX-222$_i$ peak I_{Na} was blocked by 89% ± 3% (n = 4), and in the presence of 1 mM QX-222$_i$ I_{Na} was blocked by 96% ± 5% (n = 4). The lower dose (0.5 mM) was chosen for illustrative purposes because at the higher dose <5% of the current remained.·

We compared the time course of the phasic block of peak I_{Na} to the phasic reduction of charge by fitting the reduction in peak I_{Na} and the reduction of charge during trains with the sum of exponentials. Under control conditions the reduction in peak I_{Na} in the 10 Hz pulse trains was better described with two exponentials than with one (8 of 10 cells). The faster time constant was less than two pulses and probably resulted from incomplete recovery from inactivation during the short interpulse interval. The second time constant, when present, was always >38 pulses and often longer than 100 pulses, which meant it was not well estimated by the 130 pulse train. In the presence of QX-222$_i$ the time course of the block of peak I_{Na} also contained the fast time constant associated with incomplete recovery. A second time constant in the presence of 0.5 mM QX-222$_i$, which represented the phasic block by the drug, was 10.2 ± 3.3 pulses (n = 4). Block developed only slightly faster with 1 mM QX-222$_i$ (7.7 ± 2.1 pulses, n = 6), and the time constant was not statistically different from that in 0.5 mM drug.

In the presence of QX-222$_i$ the reduction in charge during trains was best described by a single time constant. We did not observe a reduction in charge that paralleled the rapid decrease in peak I_{Na} that was seen both in control and in the presence of drug. The time constants of reduction in charge for 0.5 or 1 mM QX-222$_i$ were not different and had a mean value of 11.8 ± 7 pulses (n = 10). This time constant corresponded closely to that for block of I_{Na} and suggests that block of I_{Na} is directly related to the reduction in gating charge for cardiac Na channels.

The gating current remaining at the end of the train presumably represents predominantly the voltage-dependent gating of drug-bound channels because (a) virtually all of the ionic current was blocked by the drug, and (b) we have previously shown that the nonlinear capacitative currents under our experimental conditions in single canine cardiac Purkinje cells almost entirely represent the gating of Na channels (Hanck et al., 1990). By examining the time constants of I_g relaxations we should be able to know whether gating is altered in the presence of quaternary lidocaine.

We, therefore, analyzed the time constants of I_g relaxations in 10 cells exposed to 0.5 and 1 mM QX-222$_i$. Individual sweeps from the pulse trains were capacity corrected, trimmed, decimated by two, and fit with up to three exponential terms. As expected, at this potential most of the relaxations were best described by a single exponential. In those sweeps in which a second time constant was detected (only 14 of 78), the second τ was about 10 times longer, 2.2 ms ± 1.6 ms, with an initial amplitude only 6% ± 5% of the amplitude of the dominant time constant. Summary data are presented graphically in Fig. 4. Under control conditions there was a small increase in the initial amplitude of I_g (Fig. 4 A) and a concomitant decrease in the time constant of I_g relaxation (Fig. 4 B). These effects paralleled the rapid, small reduction in peak I_{Na} observed (Fig. 3) that was attributed to incomplete recovery from inactivation. In the presence of QX-222$_i$ the initial amplitude of I_g became

progressively smaller during the train (Fig. 4*A*) as did the time constant of I_g relaxation (Fig. 4*B*). The phasic reduction in charge during the pulse train could be accounted for by an about equal reduction in the time constant and the initial amplitude; the time constant shortened by 22% and the initial amplitude was reduced by 27%. Therefore, consistent with the modulated-receptor hypothesis, block of I_{Na} by QX-222$_i$ was associated with altered Na channel kinetics.

Effect of QX-222$_i$ on the Voltage Dependence of Channel Kinetics

We characterized the voltage dependence and kinetics of the gating currents from drug-bound Na channels by measuring current-voltage and charge-voltage (Q-V) relationships immediately following pulse trains in which most of the channels became drug-bound. 10 s after producing channel blockade with 130 pulse 10 Hz trains, cells were depolarized to a series of potentials over the range Na channels activate. Four depolarizations to each test potential were made both for I_{Na} and I_g measurements. Data from a representative cell in which I_{Na} was measured after exposure to 0.5 mM QX-222$_i$ are shown in Fig. 5. Data from this concentration, rather than those after exposure to 1 mM QX-222$_i$, are shown because a sufficient amount of current remained for illustrative purposes. Peak I_{Na} for each of the four depolarizations are plotted at each test potential in order to demonstrate that there was little additional block or recovery from block during the voltage protocol. In two cells (1 mM QX-222$_i$) we looked specifically at the difference in block at the beginning and end of the I_{Na}-V protocol; in one cell peak Na currents were identical and in the other there was 5% less current in the last pulse in the protocol. It should be noted, however, that during the interval between the end of the pulse train and the beginning of the I_{Na}-V protocol there was a small amount of recovery that was about proportional to the fast component of reduction in I_{Na} that occurred during the train. In two cells exposed to 1 mM QX-222$_i$ we compared peak I_{Na} at the end of train to the peak I_{Na} recorded during the I-V protocol; average current remaining at the end of the pulse train was 6%, and it increased only to 10% over the 1 min between the train and the end of the I_{Na}-V protocol. Therefore, only minimal recovery from block occurred between the pulse trains and the subsequent I_{Na}-V protocols and during the I_{Na}-V protocols.

Following the same protocols as above but with all Na$^+$ replaced by TMA$^+$ and STX added to the bath, I_g were recorded (Fig. 6). Consistent with the data from pulse trains, which indicated that drug-bound channels gated with altered kinetics, the time course of I_g was altered over the entire potential range. Note that the initial amplitude of the smallest I_g in QX-222$_i$ at the most negative potential (−120 mV) was larger than the smallest I_g in control while the initial amplitude in QX-222$_i$ at the most positive test potential (30 mV) was smaller than that in control. More strikingly, I_g relaxed more rapidly over the entire voltage range after exposure to QX-222$_i$.

We analyzed the decays of I_g (0 Na$^+$ and 10 µM STX) as a function of voltage after trains in six cells in control and in the presence of 1 mM QX-222$_i$, a dose in which, based on I_{Na} measurements, >90% of the channels were blocked. In each case between 30–60 µs of data were trimmed, data were decimated by two, and were fit with up to three exponential components. Means ± SEM of the time constants and initial amplitudes are shown in Fig. 7. We have previously shown that under control
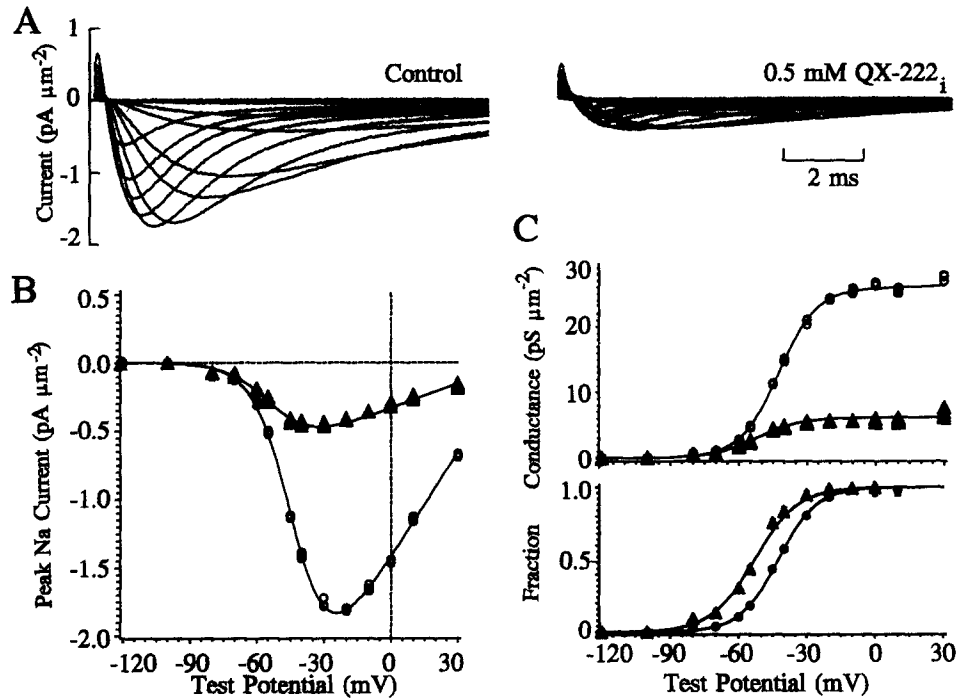
FIGURE 5. Voltage dependence of I_{Na} after 130 pulse, 10 Hz trains to 0 mV. 10 s after a pulse train at 10 Hz, step depolarizations (four replicates) over a range of potentials from a holding potential of −150 mV were recorded. (*A*) Capacity and leak corrected raw data from single sweeps in control (*left*) and in the presence of 0.5 mM QX-222$_i$ (*right*) during 10 ms steps to −120, −100, −80, −70, −60, −55, −45, −40, −30, −20, −10, 0, +10, and +30 mV. For graphing data were digitally filtered at 5 kHz and only every sixth point was plotted. (*B*) Peak I_{Na} vs. voltage for the same cell in control (O) and in the presence of QX-222$_i$ (▲). Note the similarity between peak currents in each of the four replicates. Solid line is the fit to the data of a modified form of a Boltzmann distribution:

$$I = \frac{(V_t - V_{rev})\, G_{max}}{1 + e^{(V_t - V_{1/2G}/s)}} \tag{1}$$

where I is the peak current in the depolarizing step and V_t is the test potential. The parameters estimated by the fit were V_{rev}, the reversal potential, G_{max}, the maximum peak conductance, $V_{1/2G}$, the half-point of the relationship, and s, the slope factor in mV's. Parameters of the fits were as follows:

Condition	G_{max}	s	$V_{1/2G}$	V_{rev}
	$pS\ \mu m^{-2}$		mV	
Control	26	−8.5	−43	55
0.5 mM QX-222$_i$	6	−9.6	−52	55

(*C*) Conductance transforms of the data in *B*. Lower panel shows the data normalized to emphasize that the slope factor was similar after exposure to drug. The difference in half-point of the relationship was that expected from the background shift in kinetics (Hanck and Sheets, 1992). Cell E7.03; R_L 56 MΩ; 101 pF; 14°C.

conditions over most of the voltage range the decay of I_g was usually fit best by two exponentials; the slower time constant with the larger initial amplitude had a biphasic dependence upon potential while the faster time constant, which was in the range of 0.1 ms, made a small contribution to charge (Hanck et al., 1990). The second, faster time constant was not found routinely in these experiments, which may have been because we used TMA^+ rather than Cs^+ as the intracellular cation. Because TMA^+ is less conductive than Cs^+, the rising phase of I_g was slightly longer in these experiments, making detection of this small, rapid component more difficult. The second time constant under control conditions had an amplitude less than 10% of the amplitude of the dominant time constant and was not very voltage dependent (Fig. 7, C and D).

In the presence of 1 mM $QX-222_i$ there was a dramatic abbreviation of the dominant time constant (Fig. 7 A). Rather than having a biphasic dependence on
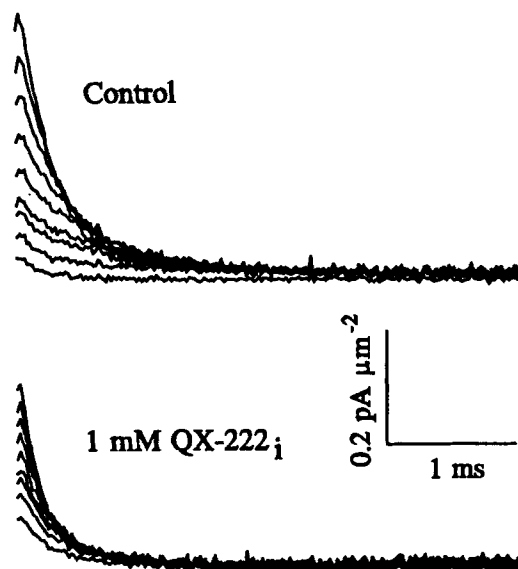

FIGURE 6. Time course of I_g during step depolarizations to −70, −55, −45, −40, −30, −20, −10, 0, and +10 mV and 10 s after a 130-pulse 10 Hz train in control (*upper*) and in 1 mM $QX-222_i$ (*lower*). Data are shown capacity, but not leak, corrected digitally filtered at 20 kHz with only every sixth point plotted. Twenty-four samples were removed from the beginning of each sweep to eliminate the filtering artifact. Cell K2.04; R_L 125 MΩ; 95 pF; 13.8°C.

potential it appeared to monotonically decrease and to change much less as a function of voltage than in control. After exposure to drug, at potentials negative to −40 mV, the initial amplitude of the dominant I_g was greater while at more positive potentials it was less after exposure to drug (Fig. 7 B, also see Fig. 6).

The mean Q-V relationship and the fits of a Boltzmann distribution to the data are shown in Fig. 8 for six cells before and after exposure to 1 mM $QX-222_i$. In addition to a reduction in Q_{max} from 0.29 ± 0.08 fC μm^{-2} to 0.16 ± 0.03 fC μm^{-2}, the Q-V relationship of drug-bound channels was shifted to more negative potentials, and it had a less steep voltage dependence compared to control. Although a Boltzmann distribution, which describes the voltage-dependent transfer of charge between two kinetic states, is an oversimplification of channel kinetics, we have previously shown that the half-points from the charge-voltage relationship and peak conductance-voltage relationship are similar under control conditions in this cell type suggesting

that charge is concentrated near the opening transition for this isoform of the channel (Hanck et al., 1990). The half-point for six cells exposed to 1 mM QX-222$_i$ was shifted by -27 ± 6 mV, from -56 ± 5 mV to -82 ± 9 mV, and the slope factor was reduced from -9.6 ± 1.8 mV to -18.2 ± 1.5 mV. The change in slope factor and
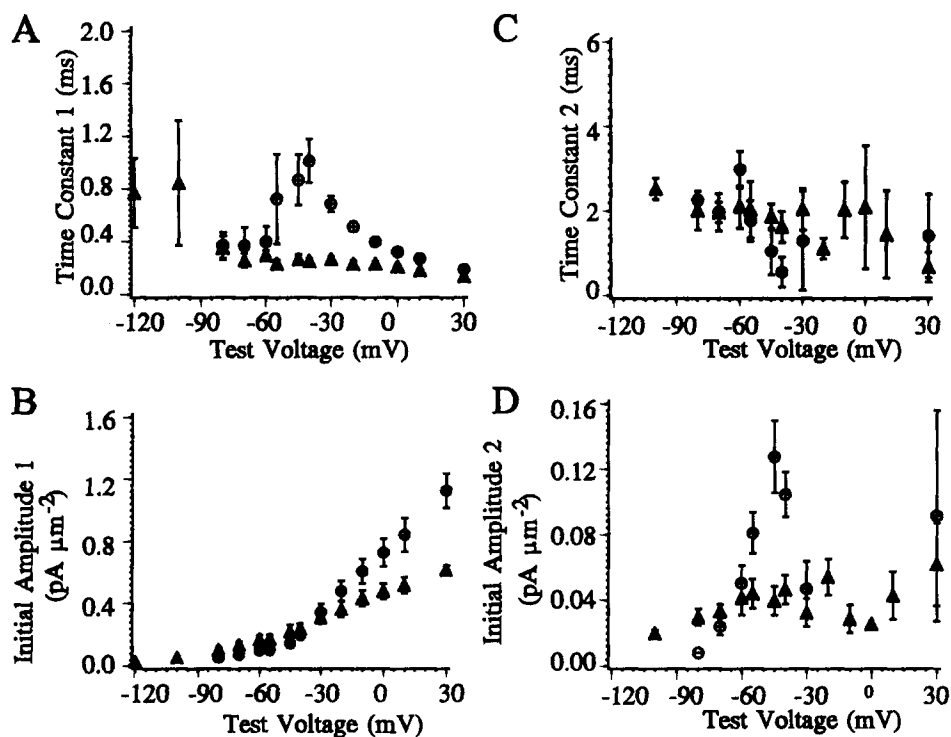

FIGURE 7. Voltage dependence of I$_g$ relaxations in control (○) and in the presence of 1 mM QX-222$_i$ (▲). Data are shown as means and SEM for each of the parameters from the fits to paired measurements of I$_g$ relaxations in six cells. Data were fit with a sum of exponentials as described in the text and segregated according to the initial amplitude contribution of each time constant. In the majority of cases (86 of 153 signal-averaged traces) data were best described by two time constants (31 control, 55 drug), and these data are graphed with the time constant contributing the larger amplitude as τ1 (A, B) and the smaller amplitude as τ2 (C, D). In 54 of 153 cases I$_g$ relaxations were best described by a single time constant (35 control, 19 drug). Such cases were concentrated at the more positive potentials (≥ -20 mV), and these data are included in the left panels (A, B). In only 13 of 153 cases were three time constants detected (five control, eight drug). In these cases two of the three time constants were similar to the ones detected when data were best described by two time constants and the third was faster (0.1 ms ± 0.04 ms). The results from the two time constant fits were graphed in such cases.

half-point can be better appreciated in B. Because fewer than 10% of the channels remained unblocked by drug, this relationship was taken to represent the Q-V relationship of drug-bound channels (also see below). It should be noted that the data overestimate the shift in half-point produced by QX-222$_i$ by about 5–10 mV

because of the known background shift in kinetics (Hanck and Sheets, 1992, and see below).

The reduction in slope factor implied that the gating of drug-bound channels was less voltage dependent than drug-free channels. Whereas valency for control channels was about 2.5 e^-, valency for drug-bound channels was about 1.3 e^-. This reduction in voltage dependence (i.e., slope factor) of the gating would itself be expected to reduce Q_{max} because Q_{max} is a determined by the product of the total number of Na channels gating and the valence of each channel. After block was produced by 1 mM QX-222$_i$ the voltage dependence of the Q-V relationship was
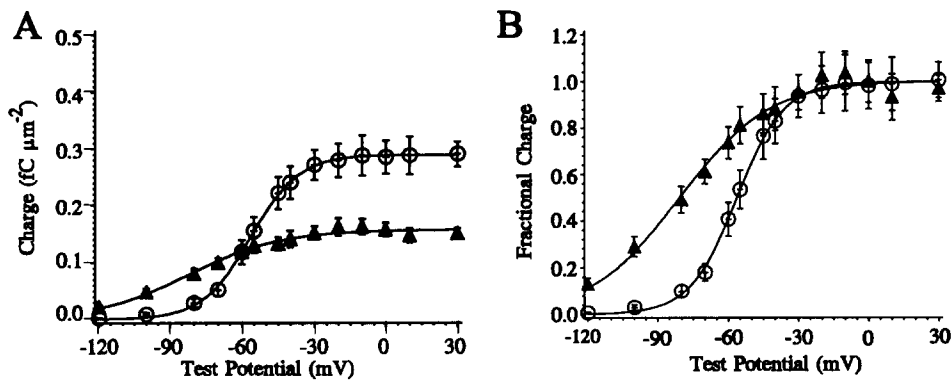

FIGURE 8.   Voltage dependence of charge in control (O) and after exposure to 1 mM QX-222$_i$ (▲) for six cells. Solid lines are the means of the parameters estimated from the fits to each data set of a Boltzmann distribution:

$$Q = \frac{Q_{max}}{1 + e^{V_t - V_{1/2}/k}} \tag{2}$$

where charge (Q) transferred during depolarizations to various voltages (V_t), was expressed relative to the maximum charge (Q_{max}). Parameters estimated by the fit were Q_{max}, the voltage of the half-point of the relationship ($V_{1/2}$), and the slope factor (k), expressed in mV's. Values are given in the text. (*B*) Same data as *A* except data are shown normalized to better illustrate the shift in half-point, which was much greater than expected from the background shift in kinetics (Hanck and Sheets, 1992, also see Fig. 12 and text), and the reduction in the slope factor.

reduced to 53% ± 10% of that in control. The reduction in Q_{max} to 56% ± 10% was, therefore, accounted for by the reduction in valency. Had a fraction of the channels gated too slowly to be measured or not gated at all, i.e. become immobilized, this should have been manifested as an additional reduction in charge beyond that attributable to the reduction in voltage dependency. We, therefore, found no evidence under our experimental conditions for immobilization of charge for drug-bound channels.

If this interpretation of the data is correct, then we would expect that as the number of channels blocked by QX-222$_i$ were varied, the charge-voltage relationship

would reflect the relative contributions of the gating of the two populations, drug-free and drug-bound channels. To test this hypothesis we took advantage of the slow development of block at low concentrations. The protocol is illustrated in Fig. 9. After obtaining control measurements cells were exposed to 0.05 mM $QX-222_i$ and pulsed to 0 mV for 10 ms at 10 Hz to develop block of I_{Na}. After various amounts of partial block of I_{Na} developed, the pulse trains were interrupted and current-voltage relationships and charge-voltage relationships (replacing Na^+ by TMA^+ and the adding STX to the bath) were obtained. During these protocols the stimulation frequency was decreased to 1 Hz. For both measurements of I_{Na} and I_g there were four depolarizations to each potential, and for charge measurements data were signal-averaged.

With the additional block of I_{Na} that developed in each train, the conductance-voltage relationships were scaled downward (Fig. 10 A). G_{max} was reduced but the voltage dependence of conductance (slope factor) was unaffected. This was as would be expected for a condition in which blocked channels were nonconducting and little block or recovery from block occurred during the protocol; the conductance-voltage relationship reflected only the response of unblocked channels. The small shift in the half-point of the conductance-voltage relationship to more negative potentials resulted from the time-dependent shift in cardiac Na channel kinetics during the course of the measurements (Hanck and Sheets, 1992).

For the charge-voltage relationship, Q_{max} also became smaller, but as the number of channels blocked by $QX-222_i$ increased, the Q-V relationship became progressively less steep and the half-point of the relationship shifted to more hyperpolarized potentials (Fig. 10 B). This presumably occurred because charge reflected the gating of all channels, both blocked and unblocked, and at each test point the Q-V relationship represented a greater proportion of channels that were gating with altered kinetics.

Consistent with this interpretation, there was a high degree of correlation between Q_{max} and G_{max} (Fig. 11 A), which predicted that when all channels were blocked by drug that 52% ± 3% of the charge would remain. This value was similar to the mean value from the previously described data with 1 mM $QX-222_i$ and gave independent evidence that the kinetics observed in 1 mM $QX-222_i$ represented the gating of drug-bound channels. We would also expect that the charge-voltage relationships would reflect the varying contributions of drug-free and drug-bound channels, i.e., be described as double Boltzmann distributions. However, we should recognize that a single Boltzmann distribution is an approximation to the data even under control conditions and, more importantly, because the differences in the half-points (~ 27 mV) and voltage dependence (reduction of valence by $\sim 50\%$) between the populations were rather modest, the detection of the predicted double Boltzmann by fitting would be difficult. This is illustrated in Fig. 11 B, which shows simulated datasets based on the mean values from the grouped data for control and 1 mM $QX-222_i$. The solid lines represent the fits of the simulated double Boltzmann relationships to single Boltzmann distributions. Although detection of the double Boltzmann parameters in the charge distributions was not practical, the Q-V relationships should become less steep and Q_{max} should decrease as the proportion of drug-bound channels is increased, such that the parameters from single Boltzmann fits would be
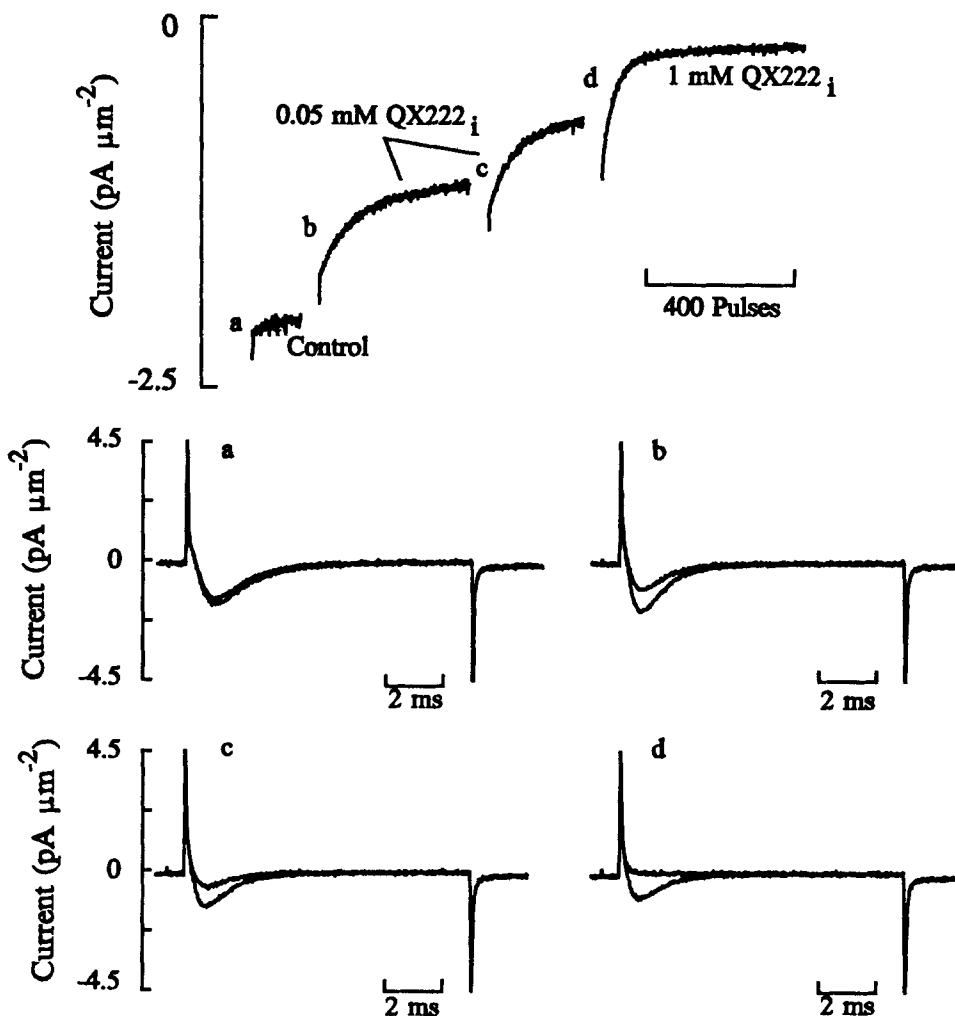
FIGURE 9. Blockade of I_{Na} produced by 0.05 mM and 1 mM QX-222$_i$. Upper trace shows peak I_{Na} vs time. Cell was pulsed at 10 Hz to 0 mV to produce blockade of the channels. Rapid pulsing was discontinued at intervals for determination of conductance-voltage and charge-voltage relationships. Lower panels show superimposed responses of the first and last depolarizations recorded during the intervals labeled. Data are shown neither capacity nor leak-corrected. It should be noted that during the long trains of pulsing, an additional time constant in the development of block was apparent at both concentrations. During interval b, reduction in peak I_{Na} was best described by two blocking terms: τ_1 54 pulses, A_1 0.57 pA μm^{-2}; τ_2 267 pulses, A_2 0.55 pA μm^{-2}. During interval c, only one blocking τ was detected, 73 pulses with amplitude 0.92 pA μm^{-2}. During interval d, when the cell was exposed to 1 mM QX-222$_i$, again two time constants of block were detected: τ_1 30 pulses, A_1 1.09 pA μm^{-2}; and τ_2 271 pulses, A_2 0.19 pA μm^{-2}. Cell K4.03; 145 MΩ; 89 pF; 13°C.

highly correlated. In keeping with this expectation, there was a high correlation between the reduction in Q_{max} and the reduction in the slope factor (Fig. 11 C). The curved line is the relationship that would have been expected based on the grouped statistics. Note that not only is the high degree of correlation present, but the prediction that the data points should fall to the left of or on the line of identity
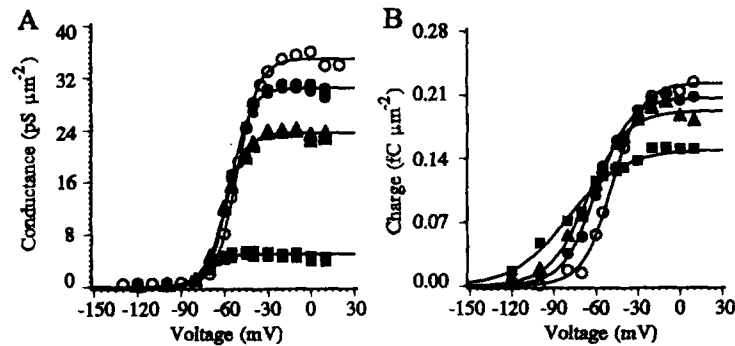

FIGURE 10. Conductance-voltage and charge-voltage relationships during blockade of Na channels by QX-222$_i$ (same cell as Fig. 9). (A) Conductance-voltage relationships determined 10 s after discontinuing pulsing. The background shift in kinetics, calculated from the change in half-points with time, was 0.8 mV min^{-1} ± 0.1 mV min^{-1}. Solid lines were calculated from the parameters from fits of the Boltzmann transform to the current-voltage data as follows:

Condition	G_{max}	s	$V_{1/2G}$	V_{rev}
	$pS\ \mu m^{-2}$		mV	
Control (a, O)	31	−7.4	−51	50
0.05 mM QX-222 (b, ●)	26	−7.2	−56	49
0.05 mM QX-222 (c, ▲)	21	−7.5	−60	49
1.0 mM QX-222 (d, ■)	5	−7.3	−72	40

(B) Charge voltage relationships determined immediately after the conductance-voltage relationship at the times indicated by the interruptions in pulsing in Fig. 9.

Condition	Q_{max}	k	$V_{1/2}$
	$fC\ \mu m^{-2}$		mV
Control (a, O)	0.22	−10.7	−48
0.05 mM QX-222 (b, ●)	0.21	−11.9	−60
0.05 mM QX-222 (c, ▲)	0.19	−13.9	−65
1.0 mM QX-222 (d, ■)	0.15	−19.5	−79

($straight\ line$) is also borne out by the data. Similarly, when the slope factors, rather than the fractional reduction in slope factor, is plotted as a function of blocked channels, i.e., reduction in G_{max}, the data match the expectation based on the grouped data (Fig. 11 D).

To rule out that the effect we observed was not an effect of time on the experimental preparation, Q-V relationships from each of three cells in control
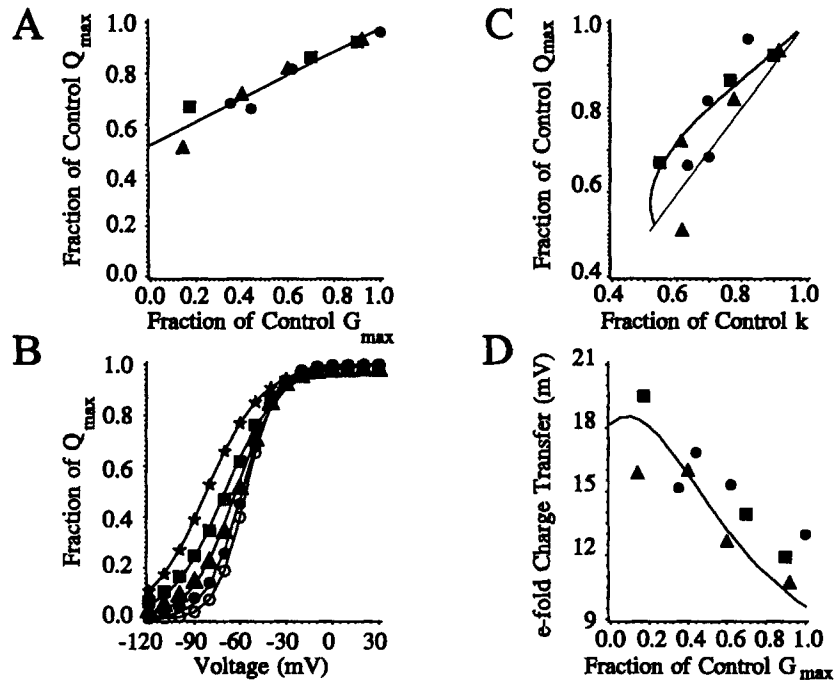
FIGURE 11. Changes in gating parameters as an increasing fraction of the channels were blocked by QX-222$_i$ in the manner described in Fig. 9. Data are from three cells: K4.01 (⊖) 90 MΩ, 134 pF, 13.5°C; K4.02 (▲) 187 MΩ, 74 pF, 13°C; Cell K4.03 (▦) 145 MΩ; 89 pF; 13°C. (*A*) Reduction in Q_{max} was directly proportional to the number of Na channels blocked by QX-222$_i$ as assessed by the reduction in G_{max}. Solid line is the result of linear regression with a slope of 0.47 ± 0.08 and an intercept of 0.52 ± 0.03 (R^2 = 0.91). Note that the predictions of the regression on paired measurements made in three cells were similar to those from the cells exposed to 1 mM QX-222$_i$. (*B*) Simulations of populations of drug-blocked and drug-free channels, assuming Boltzmann parameters from the data shown in Fig. 8 when the population was drug-free (○), 25% drug-blocked (⊖), 50% drug-blocked (▲), 75% drug-blocked (▦), and 100% drug-blocked (★). Solid lines are the fits of these data to single Boltzmann distributions. (*C*) Reductions in Q_{max} were directly proportional to reductions in slope factor for the fit to single Boltzmann distributions. The curved line shows the expectation based on the fits of simulated data, as in *B*, to single Boltzmann distributions. Consistent with the expectation that the relationships represented the sum of gating of two distinct populations, there was a high degree of correlation between the reduction in Q_{max} and the reduction in slope factor, and the data predominantly fell to the left of the line of identity (*straight line*). (*D*) The slope factors from the Boltzmann fits to the data as a function of the fraction of unblocked channels as estimated by the relative magnitude of G_{max}. The line illustrates the relationship expected from the simulations. The fact that the data fall above the line near the G_{max} maximum probably resulted from the fact that the control slope factor for these cells was slightly less than that for the mean data (10.5 mV vs. 9.6 mV). It is possible that we have slightly overestimated the reduction in slope factor produced by QX-222$_i$ because the relationship of slope factor to fraction of blocked channel contains a slight "hook" in the relationship in the range of block we observed for 1 mM QX-222$_i$. However, the experiments were not designed to test for such a hook and the error in our assumption that the values in 1 mM represent the fully modified condition appear to be quite small, i.e., the match with the data is quite good.

solutions were recorded 22.5, 26, and 27 min apart (Fig. 12). This was about twice the difference in time between control and QX-222$_i$ measurements (13 ± 3.3 min, n = 6). There was no significant change in Q$_{max}$ with time (0.24 ± 0.03 fC μm^{-2} and 0.24 ± 0.01 fC μm^{-2}). As expected from the background shift in kinetics seen in these cells (Hanck and Sheets, 1992), over this time period the half-point shifted from −50 ± 2.7 mV to −70 ± 1.7 mV. Even though the relationship shifted by 20 mV, the voltage dependence of charge was similar −11.6 ± 3.0 mV and −13.1 ± 2.3 mV respectively. It should be noted, however, that although the difference in slope factor was not statistically significant, we have observed a reduction in the slope factor of the Q-V relationship at very late times (data not shown). These data demonstrate that the changes in the Q-V relationship after QX-222$_i$ did not result from an effect of time on our experimental preparation.

We considered the possibility that the reduction in Q$_{max}$ and slope factor by QX-222$_i$ resulted from the permanently charged drug moving counter to the channel's voltage sensor, thereby producing only an apparent decrease in Na channel gating valence. To investigate this possibility, I$_g$ was recorded after exposure to the
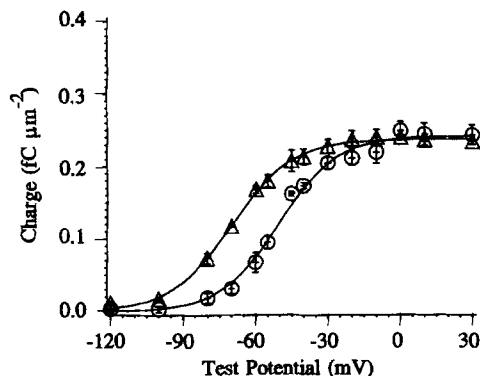

FIGURE 12. The effect of the background shift in kinetics on the charge-voltage relationship. Data shown are the means ± SEM for three cells in which no experimental intervention was made, but in which measurements were made 22.5, 26, and 27 min apart (1st ○, 2nd △). Solid lines were calculated from the means of the parameters determined by the fits of a Boltzmann distribution to the individual datasets. Values are given in the text.

uncharged local anesthetic drug, benzocaine. Because of the low solubility of benzocaine in water, 2 mM was the highest concentration that could be studied. Protocols similar to those used for the study of QX-222$_i$ were used. Conductance-voltage relationships were recorded, 2 mM benzocaine was added to the bath, and after several minutes a 130-pulse, 10 Hz train with 10 ms depolarizations to 0 mV from a holding potential of −150 mV was applied followed by an I-V and Q-V determination. An example of the effect of benzocaine on the conductance-voltage relationship and the charge-voltage relationship is shown in Fig. 13. In two cells peak conductance was reduced by 65% (mean) without a significant change in slope factor or half-point. After replacement of Na$^+$ by TMA$^+$ and the addition of STX to the bath, a charge-voltage relationship was obtained. In two cells mean reduction in Q$_{max}$ was 21% (0.24 fC μm^{-2} to 0.19 fC μm^{-2}), and this was accompanied by a reduction in the slope factor of the Boltzmann fit to data from −11.7 to −14.6 mV and a shift in the half-point from −52 to −63 mV (mean, n = 2). Because the effect of benzocaine was reversible, we could confirm that the charge-voltage relationship returned towards normal after wash-out of the drug. Even though 2 mM benzocaine did not

block all the Na channels, the changes in the charge-voltage relationship were similar to those caused by $QX222_i$. We, therefore, believe that it is unlikely that the reduction in slope factor or the shift of the charge-voltage relationship in the presence of $QX-222_i$ was secondary to the charge of the drug moving counter to the Na channel's voltage sensor.
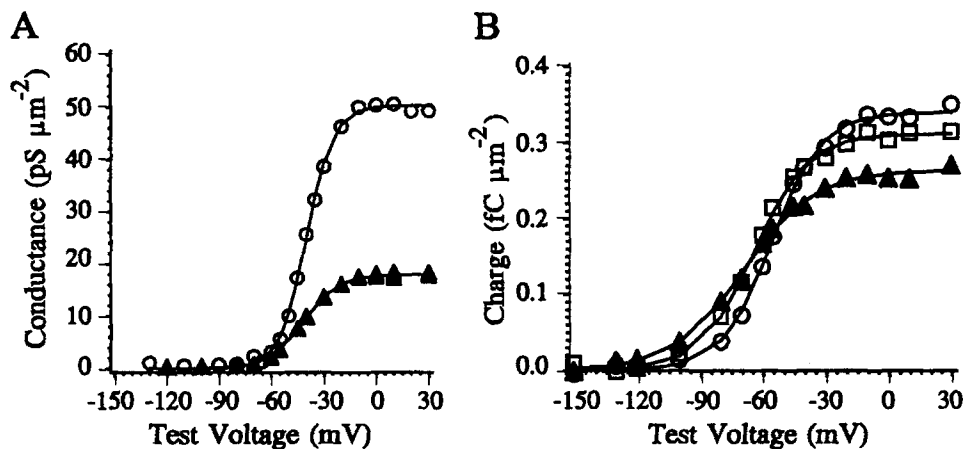

FIGURE 13. Effect of 2 mM benzocaine on Na channel conductance and charge after a 130-pulse, 10 Hz train. (*A*) Conductance-voltage relationship in control (○) and after benzocaine (▲). The parameters estimated by the fit of the Boltzmann transform were as follows:

Condition	G_{max}	s	$V_{1/2G}$	V_{rev}
	$pS\ \mu m^{-2}$		mV	
Control	50	−7.7	−40	55
2 mM Benzocaine	18	−9.8	−42	55

(*B*) Charge-voltage relationship in control (○), after benzocaine (●) and after wash (□). The parameters estimated by the fit of a Boltzmann distribution were as follows:

Condition	Q_{max}	k	$V_{1/2}$
	$fC\ \mu m^{-2}$		mV
Control	0.34	−12.0	−56
2 mM Benzocaine	0.26	−17.1	−69
Wash	0.31	−13.1	−64

Cell J8.01; R_L 140 MΩ; 105 pF; 14°C.

DISCUSSION

We have provided evidence, based on the measurement of Na channel gating currents in canine cardiac Purkinje cells, that cardiac Na channels gate with altered kinetics when bound to the quarternary lidocaine derivative, QX-222, and the neutral local anesthetic, benzocaine. However, of even greater interest is our finding that

channels bound to drug, rather than becoming stabilized in an immobilized or nongating conformation, continue to gate, but with lesser voltage dependency than drug-free channels. We, therefore, suggest a new interpretation of the modulated receptor hypothesis, whereby drug may prevent full movement of the voltage sensor.

Interaction Between Quarternary Lidocaine and Guanidinium Toxins

Unlike for the neuronal forms of the Na channel, which have been previously investigated (Cahalan and Almers, 1979b; Guselnikova et al., 1979; Khodorov, 1981), in these studies, phasic reduction of charge was not affected by the presence of guanidinium toxin. While we cannot exclude the possibility that our choice of STX over TTX, which is the toxin used in the previous studies, or that our choice of QX-222 rather than QX-572 or QX-314 was responsible for observed differences, we suggest that it is more likely to represent differences between the binding sites in the isoforms of the channel. Recent structure-function studies on several isoforms of the Na channel have suggested that the differences in binding affinity for STX and TTX between isoforms can be explained by small amino acid changes in homologous regions of the molecules, suggesting that the binding sites for toxins on various channel isoforms is largely conserved (Terlau, Heinemann, Stuhmer, Pusch, Conti, Imoto, and Numa, 1991; Backx, Yue, Lawrence, Marban, and Tomaselli, 1992; Satin, Kyler, Chen, Bell, Cribbs, Fozzard, and Rogart, 1992). Also the comparisons of the action of antiarrhythmic agents in various preparations have, at least so far, suggested that affinity for these agents is similar between isoforms, with differences secondary to voltage-dependent differences in lifetimes in various states (Bean, Cohen, and Tsien, 1983; Makielski and Fan, 1993). Structure-function studies will eventually help us understand how the interaction between drug and toxin differs between isoforms.

State-dependent Block by Quarternary Lidocaine

Quarternary lidocaine compounds have long been known to block preferentially open Na channels from the inside (Frazier, Narahashi, and Yamanda, 1970; Strichartz, 1973). Consistent with QX-222 having the a negligible rate of access to the closed state, little block of I_{Na} or reduction in charge was seen in the first depolarization after exposure to drug. We also observed that the off-rate of drug appeared to be very slow because recovery occurred only over minutes and because over a large range of frequencies QX-222$_i$ blocked on a per pulse basis (data not shown). The recovery that we did observe could be largely attributed to channels that became inactivated because of the short interpulse interval in the pulse trains and that were, therefore, protected by block by QX-222$_i$, which blocks predominantly to the open state.

One would expect from such a simple system that the rate of development of block would increase approximately in proportion to the concentration of drug. Although we could not detect a significant difference in the rate of development of block between 0.5 and 1 mM QX-222$_i$, at ten-fold lower concentration of 0.05 mM, block developed with pulse constants of about 50 pulses (Fig. 9) rather than the 5–10 pulse constants at the higher concentrations. Therefore, as expected, the rate of block was roughly proportional to the concentration of QX-222$_i$. We should note, however,

that, contrary to the expectation for a simple system of drug binding to a single state, there was always a very slow time constant of block that was evident in very long trains. This could be seen in Fig. 9 where a second time constant greater than 200 pulses was also present.

Kinetics of Drug-Bound Channels

The kinetics of drug-bound channels were strikingly different from those of drug-free channels. Speeding of I_g relaxations has been reported for a variety of agents in squid axon and frog node of Ranvier (Keynes and Rojas, 1974; Peganov and Khodorov, 1977; Cahalan and Almers, 1979b; Tanguy and Yeh, 1989, also see reviews Khodorov, 1981; Meves, 1990), but the voltage dependence of I_g relaxations for drug-bound channels has not been examined. Similar to neuronal preparations I_g relaxations of drug-free cardiac channels had a clear biphasic dependence on voltage, with a mid-point well-matched with the mid-point of the charge-voltage relationship, as would be expected for a two-state system (Adrian, 1978). On the other hand, I_g relaxations for drug-bound channels monotonically decreased over the entire voltage range investigated. While the mid-point of the charge-voltage relationship of drug-bound channels would have predicted a biphasic dependence of I_g relaxations centered around -80 to -90 mV, this was not observed. Because I_g relaxations were fairly rapid over the entire voltage range, our detection of faster time constants may have been hindered by our clamp speed and the small size of I_g at the most negative potentials. However, because the initial amplitude of I_g was larger at negative potentials after exposure to drug than it was in control, this seems unlikely.

Comparison with Previous Studies

The most prevalent idea about the action of local anesthetics is that drug binding stabilizes an inactivated state of the channel (Courtney, 1975; Khodorov, Shishkova, Peganov, and Revenko, 1976), and this represents the classical interpretation of the action of local anesthetics and antiarrhythmic agents according to the modulated receptor hypothesis (Hille, 1977; Hondeghem and Katzung, 1977; Butterworth and Strichartz, 1990). In keeping with the finding that inactivation produces immobilization of gating charge (Armstrong and Benzanilla, 1977; Nonner, 1980), charge immobilization by quarternary derivatives of lidocaine has been reported in squid giant axon (Cahalan and Almers, 1979b; Tanguy and Yeh, 1989) and in frog node of Ranvier (Guselnikova et al., 1979; Khodorov, 1981). General discussions of this effect, e.g. Bigger and Hoffman, 1990; Butterworth and Strichartz, 1990; Hille, 1992; Snyders, Hondeghem, and Bennett, 1992, interpret the available evidence to support the idea that the gating of drug-bound channels is shifted compared with drug-free channels, so that drug-bound, inactivated configurations are favored under many conditions. This interpretation predicts that we would have observed either a reduction in Q_{max} because of a simple shift in equilibrium (similar voltage-dependence of gating) or a reduction in Q_{max} because of a shift in equilibrium as well as a reduced voltage-dependence of gating. We indeed observed that there was a reduction in charge in the presence of $QX-222_i$. However, the amount of reduction in charge could not be interpreted as an immobilization (shift in equilibrium) because

we found that the voltage dependence of the charge was reduced by an equivalent amount. Because the magnitude of Q is determined both by the number of channels gating during the measurement and the valency of the individual gates, we instead suggest that all channels continue to gate, but with lesser voltage dependency.

It is somewhat difficult to compare the voltage-dependent effects we observed with those seen in other preparations. The charge-voltage relationship measured in the presence of QX-572 in frog node of Ranvier was less steep than control and shifted in the negative direction (Guselnikova et al., 1979; Khodorov, 1981). On the other hand, the charge-voltage relationship measured in presence of QX-314 in squid giant axon (Cahalan and Almers, 1979b; Tanguy and Yeh, 1989) was also less steep than control, but was shifted in the depolarizing direction. While these results seem somewhat different from those reported here, it should be kept in mind that methodological considerations require that these neuronal preparations are studied under partially inactivated conditions, which affects both the magnitude and kinetic characteristics of charge (Krutetskaya, Lonsky, Mozhayeva, and Naumov, 1978; Meves, 1990; Ruben, Starkus, and Rayner, 1990, 1992).

The Role of Charge of the Drug

It is not known whether the charge on QX-222 is balanced by charge on the channel when the drug is bound. If some effect of the charge were to remain, then it is possible that the drug could move counter to the voltage sensor when the channel gates thereby producing only an apparent decrease in valency. However, this is unlikely because when block was produced with the neutral local anesthetic, benzocaine, there was also a reduction in the valency of gating. It has been suggested in frog node of Ranvier that the shift in the half-point of the Q-V relationship in the presence of quarternary lidocaine occurred because of the charge on the drug. In that preparation the half-point of charge was unaltered when channels were blocked with benzocaine (Neumcke, Schwarz, and Stampfi, 1980; Khodorov, 1981). Thus, benzocaine appears to affect neuronal and cardiac channels differently, although further experiments will be necessary to confirm whether this is indeed an isoform difference.

Model Implications

The physical meaning of the reduction in valency remains to be explained. Local anesthetics may hinder or reduce the movement of each set of charged residues that contribute to I_g or perhaps may prevent the movement of only some. Alternatively, drug binding may alter the placement of the charged residues within the field so that even though movement associated with gating is similar, the vectorial contribution is less. The state transitions represented by the gating of drug-bound channels are also unknown. Clearly, the effect of local anesthetic binding to voltage-gated Na channels is strikingly different from the effect in acetylcholine receptor, where it appears that binding of drug prohibits gating (closing) of the channel (Neher and Steinbach, 1978) and from the action of strychnine, which has been shown to prevent closure of Na channels (Cahalan and Almers, 1979a). It is also quite different from the action of the guanadinium toxins, where binding has been shown to produce only a small effect on gating secondary to interactions with surface charge (Hegggeness and Starkus, 1986).

It is interesting to speculate whether drug-bound channel transitions resemble more closely drug-free activation gating or whether the transitions more closely resemble rapid transitions between inactivated states. The first possibility comes to mind easily since for modified channels the charge-voltage relationship is displaced in the negative direction compared with that for drug-free channels. On the other hand, inactivated state gating would be compatible with the findings of Armstrong and Bezanilla (Armstrong and Benzanilla, 1977), who observed in squid giant axon a shift in the nonimmobilizable gating charge of inactivated channels, and the observations of Bekkers et al. (Bekkers et al., 1984), who saw no effect of the quarternary lidocaine derivative RAD-366 or benzocaine on the nonimmobilizable fraction of gating charge.

Further study will be necessary to ascertain whether the action of these agents represents the action of a class of agents specific for the cardiac isoform of the Na channel or whether it represents a general action of local anesthetics and local anesthetic-like agents with ion channels. If the former, it may hold important information about how to design cardiac specific agents and be useful for developing an understanding of the structural basis of functional differences between channel isoforms. If the latter, it could change our basic ideas about how drugs interact with channels.

REFERENCES

Adrian, R. H. 1978. Charge movement in the membrane of striated muscle. *Annual Review of Biophysics and Bioengineering.* 7:85–112.

Armstrong, C. M., and F. Benzanilla. 1977. Inactivation of the sodium channel. II. Gating current experiments. *Journal of General Physiology.* 70:567–590.

Backx, P., D. Yue, J. Lawrence, E. Marban, and G. Tomaselli. 1992. Molecular localization of an ion-binding site within the pore of mammalian sodium channels. *Science.* 257:248–251.

Bean, B. P., C. J. Cohen, and R. W. Tsien. 1983. Lidocaine block of cardiac sodium channels. *Journal of General Physiology.* 81:613–642.

Bekkers, J. M., N. G. Greeff, R. D. Keynes, and B. Neumcke. 1984. The effect of local anaesthetics on the components of the asymmetry current in the squid giant axon. *Journal of Physiology.* 352:653–668.

Bigger, J. T., Jr., and B. F. Hoffman. 1990. Antiarrhythmic drugs. *In* The Pharmacological Basis of Therapeutics. 8th edition. A. G. Gilman, T. W. Rall, A. S. Nies, and P. Taylor, editors. Pergamon Press, New York. 840–873.

Butterworth, J. F., and G. R. Strichartz. 1990. Molecular mechanisms of local anesthesia—a review. *Anesthesiology.* 72:711–734.

Cahalan, M. D., and W. Almers. 1979a. Block of sodium conductance and gating current in squid giant axons poisoned with quaternary strychnine. *Biophysical Journal.* 27:57–74.

Cahalan, M. D., and W. Almers. 1979b. Interactions between quaternary lidocaine, the sodium channel gates, and tetrodotoxin. *Biophysical Journal.* 27:39–56.

Cahalan, M., B. I. Shapiro, and W. Almers. 1980. Relationship between inactivation of sodium channels and block by quaternary derivatives of local anesthestics and other compounds. *In* Molecular Mechanisms of Anesthesia. (Progress in Anesthesiology). Vol. 2. B. R. Fink, editor. Raven Press, New York. 17–33.

Courtney, K. R. 1975. Mechanism of frequency-dependent inhibition of sodium currents in frog myelinated nerve by the lidocaine derivative GEA 968. *Journal of Pharmacology and Experimental Therapeutics.* 195:225–236.

Frazier, D. T., T. Narahashi, and M. Yamanda. 1970. The site of action and active form of local anesthetics. II. Experiments with quaternary compounds. *Journal of Pharmacology and Experimental Therapeutics.* 171:45–51.

Guselnikova, G., E. Peganov, and B. Khodorov. 1979. Blockade of the gating currents in node of Ranvier under the action of the quaternary derivative of lidocaine (compound QX572). *Dokl. Akad. Nauk. SSSR.* 244:1492–1494.

Hanck, D. A., and M. F. Sheets. 1992. Time-dependent changes in the kinetics of the sodium current in single canine cardiac Purkinje cells. *American Journal of Physiology.* 262:H1197–H1207.

Hanck, D. A., M. F. Sheets, and H. A. Fozzard. 1990. Gating currents associated with Na channels in canine cardiac Purkinje cells. *Journal of General Physiology.* 95:439–457.

Hanck, D. A., M. F. Sheets, and J. C. Makielski. 1992. Gating charge provides evidence that local anesthetics alter gating of cardiac sodium channels. *Biophysical Journal.* 61:270a. (Abstr.)

Hegggeness, S. T., and J. G. Starkus. 1986. Saxitoxin and tetrodotoxin. Electrostatic effects on sodium channel gating current in crayfish axons. *Biophysical Journal.* 49:629–643.

Hille, B. 1977. Local anesthetics: hydrophilic and hydrophobic pathways for the drug-receptor reaction. *Journal of General Physiology.* 69:497–515.

Hille, B. 1992. Ionic channels of excitable membranes. 2nd edition. Vols. 3 and 4. Sinauer Associates, Sunderland, MA. 607 pp.

Hondeghem, L. M., and B. G. Katzung. 1977. Time- and voltage-dependent interaction of antiarrhythmic drugs with cardiac sodium channels. *Biochimica et Biophysica Acta.* 472:373–398.

Keynes, R. D., and E. Rojas. 1974. Kinetics and steady-state properties of the charged system controlling sodium conductance in the squid giant axon. *Journal of Physiology.* 239:393–434.

Khodorov, B. I. 1981. Sodium inactivation and drug-induced immobilization of the gating charge in nerve membrane. *Progress in Biophysics and Molecular Biology.* 37:49–89.

Khodorov, B. I., L. Shishkova, E. Peganov, and S. Revenko. 1976. Inhibition of sodium currents in frog Ranvier node treated with local anesthetics. Role of slow sodium inactivation. *Biochimica et Biophysica Acta.* 433:409–435.

Kniffki, K. D., E. Koppenhofer, and W. Vogel. 1976. Effects of procaine on gating and sodium currents at the nodal membrane. *Pflugers Archiv.* 365:R33.

Krutetskaya, Z. I., A. V. Lonsky, G. N. Mozhayeva, and A. P. Naumov. 1978. Two-component nature of the asymmetrical displacement currents in the nerve membrane: the kinetical and pharmacological analysis. *Tsitologiya.* 20:1269–1277.

Makielski, J. C., and Z. Fan. 1993. Phasic block of cardiac and nerve Na channels by lidocaine under uniform conditions. *Biophysical Journal.* 64:89a. (Abstr.)

Makielski, J. C., M. F. Sheets, D. A. Hanck, C. T. January, and H. A. Fozzard. 1987. Sodium current in voltage clamped internally perfused canine cardiac Purkinje cells. *Biophysical Journal.* 52:1–11.

Meves, H. 1990. The gating current of the node of Ranvier. *In* Ion Channels. Vol. 2. T. Narahashi, editor. Plenum Publishing Corp., New York. 65–121.

Neher, E., and J. H. Steinbach. 1978. Local anaesthetics transiently block currents through single acetylcholine-receptor channels. *Journal of Physiology.* 277:153–176.

Neumcke, B., W. Schwarz, and R. Stampfli. 1980. Interactions of benzocaine with Na channels in myelinated nerve. *Biophysical Structure and Mechanism.* 6(suppl):137.

Nonner, W. 1980. Relation between the inactivation of sodium channels and the immobilization of gating charge in frog myelinated nerve. *Journal of Physiology.* 299:573–603.

Peganov, E., and B. Khodorov. 1977. Gating current in the Ranvier node membrane studied by ramp potential control. *Bulletin of Experimental Biology and Medicine (U.S.S.R.)* 2:515–518.

Provencher, S. W. 1976. A Fourier method for the analysis of exponential decay curves. *Biophysical Journal.* 16:27–41.

Ruben, P. C., J. G. Starkus, and M. D. Rayner. 1990. Holding potential affects the apparent voltage-sensitivity of sodium channel activation in crayfish giant axons. *Biophysical Journal.* 58:1169–1181.

Ruben, P. C., J. G. Starkus, and M. D. Rayner. 1992. Steady-state availability of sodium channels-interactions between activation and slow inactivation. *Biophysical Journal.* 61:941–955.

Satin, J., J. W. Kyle, M. Chen, P. Bell, L. L. Cribbs, H. A. Fozzard, and R. B. Rogart. 1992. A mutant of TTX-resistant cardiac sodium channels with TTX-sensitive properties. *Science.* 256:1202–1205.

Sheets, M. F., C. T. January, and H. A. Fozzard. 1983. Isolation and characterization of single canine cardiac Purkinje cells. *Circulation Research.* 53:544–548.

Snyders, D. J., L. M. Hondeghem, and P. B. Bennett. 1992. Mechanisms of drug-channel interaction. *In* The Heart and Cardiovascular System: Scientific Foundations. 2nd Edition. Vol. 2. H. A. Fozzard, E. Haber, R. B. Jennings, A. M. Katz, and H. E. Morgan, editors. Raven Press, New York. 2165–2193.

Starmer, C. F., A. O. Grant, and H. C. Strauss. 1984. Mechanisms of use-dependent block of sodium channels in excitable membranes by local anaesthetics. *Biophysical Journal.* 46:15–27.

Strichartz, G. R. 1973. The inhibition of sodium currents in myelinated nerve by quaternary derivitives of lidocaine. *Journal of General Physiology.* 62:37–57.

Tanguy, J., and J. Z. Yeh. 1989. QX-314 restores gating charge immobilization abolished by chloramine-T treatment in squid giant axon. *Biophysical Journal.* 56:421–427.

Terlau, H., S. H. Heinemann, W. Stuhmer, M. Pusch, F. Conti, K. Imoto, and S. Numa. 1991. Mapping the site of block by tetrodotoxin and saxitoxin of sodium channel-II. *FEBS Letters.* 293:93–96.